

Quantum noise of Kramers-Kronig receiver

FAN ZHANG,¹ JIAYU ZHENG,¹ HAIJUN KANG,² XIAOLONG SU,² AND QIONGYI HE³

¹ State Key Laboratory of Advanced Optical Communication System and Networks, Frontiers Science Center for Nano-optoelectronics, Department of Electronics, Peking University, Beijing 100871, China

² State Key Laboratory of Quantum Optics and Quantum Optics Devices, Institute of Opto-Electronics, Collaborative Innovation Center of Extreme Optics, Shanxi University, Taiyuan 030006, China

³ State Key Laboratory for Mesoscopic Physics, School of Physics, Frontiers Science Center for Nano-optoelectronics & Collaborative Innovation Center of Quantum Matter, Peking University, Beijing 100871, China

xyz@optica.org

Abstract: The Kramers-Kronig (KK) receiver provides an efficient method to reconstruct the complex-valued optical field by means of intensity detection given a minimum-phase signal. In this paper, we first analytically show that the quantum noise of the KK receiver keeps the radical fluctuation of the measured minimum-phase signal the same as that of the balanced heterodyne detection, while compressing the tangential noise to 1/3 times the radical one using the information provided by the Hilbert transform. In consequence, the KK receiver achieves 3/2 times the signal-to-noise ratio of balanced heterodyne detection, while presenting an asymmetric quantum fluctuation distribution depending on the time-varying phase. This provides a feasible scheme for compressing the fluctuations of the component requiring to be measured more accurately to 1/6 under the strong carrier wave condition, which is even lower than 1/4 resulted by measuring a coherent state physically. Finally, the analytic conclusions are proved by simulation results.

© 2021 Optica Publishing Group under the terms of the [Optica Publishing Group Open Access Publishing Agreement](#)

1. INTRODUCTION

Optics receiver can be categorized as two basic schemes of coherent and direct detections [1]. Coherent receiver can either use homodyne or heterodyne detection to retrieve the complexed full field information of the received signals. In contrast, direct detection can only obtain the signal intensity due to the square-law principle. Recently, an advanced concept of Kramers-Kronig (KK) receiver was proposed [2, 3], which can reconstruct the complex-valued optical field by means of intensity detection given a minimum phase (MP) signal. For KK receiver applied on the MP signal, the amplitude waveform determines its corresponding phase waveform uniquely up to a constant phase offset. The physical mechanism is that the logarithm of the signal intensity and phase are related to each other through the KK relations that apply to the signals that are causal in time. For a MP signal, it contains a data-carrying signal and a reference component that is a continuous-wave (CW) tone. When the spectrum of the signal's complex envelope is entirely above or below the reference frequency, which is so called single-sideband (SSB) signal, then a necessary and sufficient condition to be of minimum phase is that its time-domain trajectory never encircles the origin of the complex plane. From the point of the configuration, the KK receiver is equivalent to heterodyne detection with one single photodetector (PD). Due to the fact that the receiver optical front-end consists of a single photodetector, the KK receiver is particularly suitable for low-cost data center interconnect and metro-haul applications [4]. In this way, high baud rate quadrature amplitude modulation (QAM) signal can be detected using a single PD at the receiver. The latest work has achieved a net data rate per channel above 400 Gb/s with a 64 QAM signal at 85 Gbaud with a single PD KK receiver [5].

Quantum noise, which comes from the uncertainty principle of quantum variables, sets a limitation for the signal-to-noise (S/N)

ratio in the measurement of optical signal in optical communication and it is connected to quantum measurement and quantum information. In quantum information with continuous variables, the information is encoded in the amplitude and phase quadratures of optical modes and measured by homodyne or heterodyne detection [6-10]. For heterodyne detection, a simultaneous measurement of two noncommuting quantum observables introduces excess noise that originates from vacuum fluctuations of the field, which imposes a fundamental limit on the S/N ratio [11]. KK receiver offers a simultaneous measurement of the in-phase and quadrature components of the optical field, which corresponds to the amplitude and phase quadratures of an optical mode in quantum optics. A natural question is how about the quantum noise of the KK receiver?

In this paper, we study the quantum mechanical nature of the KK receiver and elucidate the fundamental relation between KK and conventional heterodyne detection. The result shows that the KK detection has the same S/N performance as that of the general heterodyne detection but with an asymmetric fluctuation distribution reflected in the position of the end point of the retrieved signal, which is different from that of the heterodyne detection. In this case, quantum noise of the KK receiver is time dependent for the in-phase and quadrature operators of an optical field, which corresponds to the amplitude and phase quadratures of an optical mode in quantum optics. Our result indicates the quantum noise limit of the KK receiver when it is used to measure the coherent state.

2. QUANTUM MECHANICAL FUNDAMENTALS OF COHERENT STATE

For optical transmission, information is conveyed by electromagnetic wave packets those are quantum states of the

electromagnetic field. A signal carried by the coherent state $|\alpha_s\rangle$ is the eigenfunction of the photon annihilation operator \hat{a} , which is expressed as $\hat{a}|\alpha_s\rangle = \alpha_s|\alpha_s\rangle$. With the Hermitian conjugate operation, the creation operator satisfies $\langle\alpha_s|\hat{a}^\dagger = \alpha_s^* \langle\alpha_s|$, thus the photon number n satisfies $\langle n_s \rangle = |\alpha_s|^2$.

The non-Hermitian operator \hat{a} can be separated into two Hermitian components \hat{a}_1 and \hat{a}_2 by $\hat{a} = \hat{a}_1 + j\hat{a}_2$, which are the in-phase and quadrature field operators and satisfy the commutation relation given by $[\hat{a}_1, \hat{a}_2] = j/2$. Here, $\hat{a}_1 = \sqrt{\frac{\omega}{2h}}\hat{q}$ and

$\hat{a}_2 = \frac{\hat{p}}{\sqrt{2h\omega}}$ are essentially dimensionless position and momentum operators, which correspond to the amplitude and phase quadratures of an optical mode in quantum optics, respectively.

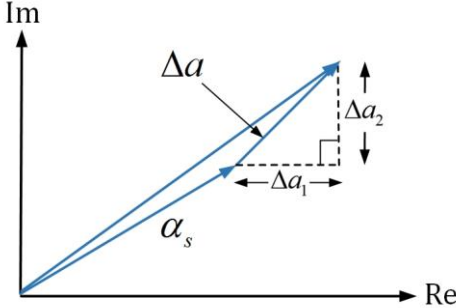


Fig. 1. The in-phase and quadrature fluctuations of the coherent state light.

The Heisenberg uncertainty principle sets an upper limit on the precision of a quantum measurement. We assume that $\langle(\Delta\hat{X})^2\rangle$ represents the quantum variance of measuring the observable \hat{X} . The coherent state is one of the minimum uncertainty states, of which the quantum variances of the in-phase and quadrature operators are $\langle(\Delta\hat{a}_1)^2\rangle = 1/4$ and $\langle(\Delta\hat{a}_2)^2\rangle = 1/4$, respectively. Thus, the total variance is $\langle(\Delta\hat{a})^2\rangle = \langle(\Delta\hat{a}_1)^2\rangle + \langle(\Delta\hat{a}_2)^2\rangle = 1/2$ [11, 12]. The relation of $\Delta\hat{a}_1$, $\Delta\hat{a}_2$ and $\Delta\hat{a}$ is shown in Fig. 1, where $\Delta\hat{a}_1$ and $\Delta\hat{a}_2$ are the real and imaginary parts of $\Delta\hat{a}$.

The quantum variances of the amplitude and phase of a coherent state are $\langle(\Delta|\hat{a}|)^2\rangle = 1/4$ and $\langle(\Delta\hat{\phi})^2\rangle = 1/(4\langle n \rangle)$, respectively [12].

Here the photon number n satisfies $\langle n \rangle = |\alpha|^2$. For any coherent state $|\alpha\rangle$ that has a time dependence $e^{-j\omega t}$, its corresponding annihilation operator is defined as $\hat{A}|\alpha\rangle = e^{-j\omega t}\alpha|\alpha\rangle$. \hat{A} and its conjugate operator \hat{A}^\dagger obey the commutation relation $[\hat{A}, \hat{A}^\dagger] = 1$.

3. QUANTUM MECHANICS MODEL OF HETERODYNE DETECTION

As shown in Fig. 2(a), the balanced heterodyne detection is adopted to get the linear beating between the local oscillator (LO)

\hat{A}_L at frequency ω_L and the signal \hat{A}_s at frequency ω_s . The waves \hat{B}_1 and \hat{B}_2 that incident upon the two PDs are [11][13]

$$\hat{B}_1 = [\hat{A}_L + \hat{A}'_s + \hat{A}'_s - j(\hat{A}_s + \hat{A}_i)]/\sqrt{2}, \quad (1)$$

$$\hat{B}_2 = [-j(\hat{A}_L + \hat{A}'_s + \hat{A}'_i) + (\hat{A}_s + \hat{A}_i)]/\sqrt{2}. \quad (2)$$

Here \hat{B}_1 and \hat{B}_2 have considered the signal \hat{A}_s at frequency ω_s and its image \hat{A}_i at $\omega_i = 2\omega_L - \omega_s$, as well as the vacuum fluctuations \hat{A}'_s and \hat{A}'_i at these two frequency points brought by LO as shown in Fig. 2(a). The above annihilation operators $\hat{A}_s, \hat{A}_i, \hat{A}_L, \hat{A}'_s$ & \hat{A}'_i are all for single frequency points. Note that n photons are received by the photodetector within a time duration T . With the elementary charge q , the current is $\hat{I} = q\hat{n}/T$. The difference between the current collected by the two detectors is

$$\begin{aligned} \langle \hat{I}(t) \rangle_{Bal} &= k \langle \hat{B}_2^\dagger \hat{B}_2 - \hat{B}_1^\dagger \hat{B}_1 \rangle \\ &= 2k |\alpha_s \alpha_L^*| \sin(\omega_{IF} t - \arg(\alpha_s \alpha_L^*)). \end{aligned} \quad (3)$$

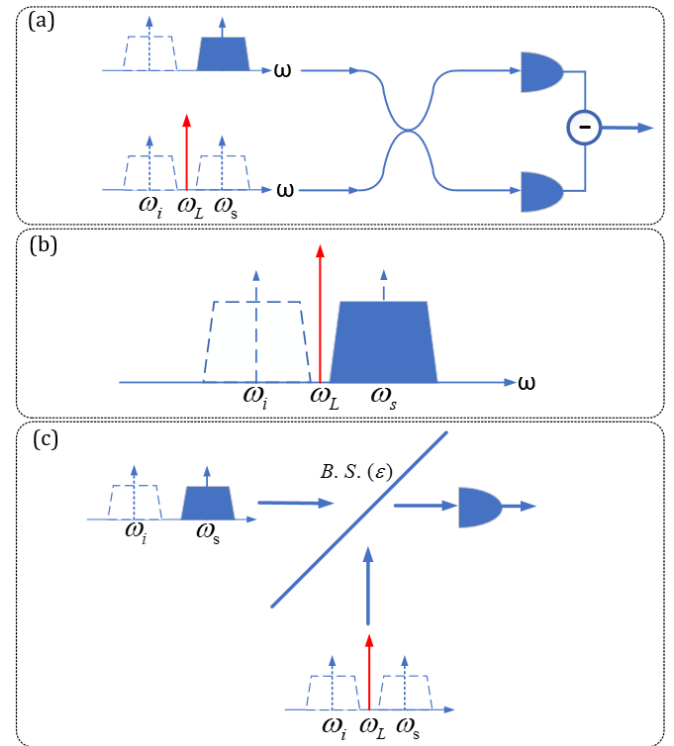


Fig. 2. Basic configurations of the balanced heterodyne and KK detection. (a) Balanced heterodyne detection; (b) The local oscillator (LO) with the signal and its image before each PD port; (c) The KK receiver.

Here $k = q/T$. α_s and α_L are the eigenvalues for the signal and the LO, respectively. $\omega_{IF} = \omega_s - \omega_L$ is the intermediate frequency. If the image band is unexcited, then $\langle \hat{A}_i^\dagger \hat{A}_i \rangle = 0$. Yet the presence of \hat{A}_i contributes to the fluctuations. The current fluctuations are

$$\langle(\Delta\hat{I})^2\rangle_{Bal} = \langle \hat{I}(t)^2 \rangle - \langle \hat{I}(t) \rangle^2 = k^2 (3\langle n_s \rangle + 2\langle n_L \rangle). \quad (4)$$

Then the S/N of the balanced heterodyne detection is calculated from Eq. (3) and (4), which is given by

$$(S/N)_{Bal} = \frac{\overline{(\langle \hat{I}(t) \rangle_{Bal})^2}}{\langle (\Delta \hat{I})^2 \rangle_{Bal}} = \frac{2\langle n_s \rangle \langle n_L \rangle}{2\langle n_L \rangle + 3\langle n_s \rangle} = \frac{\langle n_s \rangle}{1 + 3\langle n_s \rangle / \langle n_L \rangle / 2}. \quad (5)$$

Here the operation “ $\overline{\hat{X}(t)}$ ” means averaging the value $\hat{X}(t)$ by time.

4. QUANTUM MECHANICS MODEL OF THE KK RECEIVER

For the KK receiver, the signal is retrieved with one single PD of the balanced detection, which is equivalent to sending the LO along with the signal from the transmitter side as shown in Fig. 2(c). The SSB signal is constructed with a co-polarized reference carrier with real-valued amplitude and a complexed optical data. When the SSB signal impinges upon one single PD, the beating between the reference carrier and the data-carrying signal is analogue to heterodyne detection.

Without loss of generality, we express the SSB signal as $h(t) = \sqrt{1-\varepsilon}A_L + \sqrt{\varepsilon}A_s(t)$ [11], where the coupler power transmission ε is set to $\frac{1}{2}$ for balanced detection depicted as

formula (1) and (2). For the KK receiver as a means of single PD port heterodyne detection, in order to maximize the utilization of signals, we set the power transmission $\varepsilon \rightarrow 1$. We rewrite

$h(t) = [\sqrt{1-\varepsilon}\alpha_L + \sqrt{\varepsilon}\alpha_s(t)e^{-j\omega_{IF}t}]e^{-j\omega_L t}$. For a complex data-carrying signal $\alpha_s(t)$ whose spectrum is contained in the frequency range $(0, W]$, an ideal SSB signal that has its spectrum closely above the reference frequency ω_L satisfies $\omega_{IF} = \pi W$. The second-order term $\varepsilon|\alpha_s(t)|^2$ is commonly referred to as the signal-to-signal beat interference (SSBI), whose spectrum is in the frequency of $[-W/2, W/2]$ [3]. The balanced heterodyne detection can eliminate SSBI by the subtracting in Eq.(3). In contrast, for the KK receiver that with one single PD, the SSBI cancellation is not required as $\varepsilon|\alpha_s(t)|^2$ is an essential part of the detected current intensity that required for the reconstruction [3].

For each signal symbol transmitted, the purpose of KK receiver is to recover the baseband signal $\alpha_s(t)$ at the decision time t from the amplitude and phase of $h(t)$. The current $I(t) = k|h(t)|^2$ is obtained from a single PD. With the MP condition $\varepsilon\langle n_s \rangle < (1-\varepsilon)\langle n_L \rangle$ ($\varepsilon \rightarrow 1$), which means $\langle n_L \rangle \gg \langle n_s \rangle$, $\phi(t)$ is defined as the phase of $h(t)$ that can be extracted from the current logarithm with Hilbert transform [2].

$$\phi(t) = \frac{1}{2\pi} \mathcal{P} \int_{-\infty}^{+\infty} \frac{\ln |I(t')|}{t-t'} dt'. \quad (6)$$

Here \mathcal{P} represents the Cauchy principal value. The complex signal field α_s is retrieved as α'_s .

$$\alpha'_s = \left[\frac{1}{\sqrt{\varepsilon}} |h(t)| e^{j\phi(t)} - \frac{\sqrt{1-\varepsilon}}{\sqrt{\varepsilon}} \sqrt{\langle n_L \rangle} \right] e^{j\omega_{IF}t}. \quad (7)$$

Considering that $\varepsilon \rightarrow 1$, The relation between α'_s and $h(t)$ is shown in Fig. 3.

From Eq. (7), the relation between $\Delta\hat{\alpha}'_s$ and $\Delta\hat{h}$ is given by a down conversion as Eq.(8).

$$\Delta\hat{\alpha}'_s = \Delta\hat{h} e^{j\omega_{IF}t}. \quad (8)$$

It is obvious that the retrieved α'_s , which can be obtained from $h(t)$ after a phase shift with an exponent translation, has the quantum noise determined by that of $h(t)$. Therefore, in the following sections, we study the quantum fluctuations of α'_s through those of $h(t)$ in the case of KK detection.

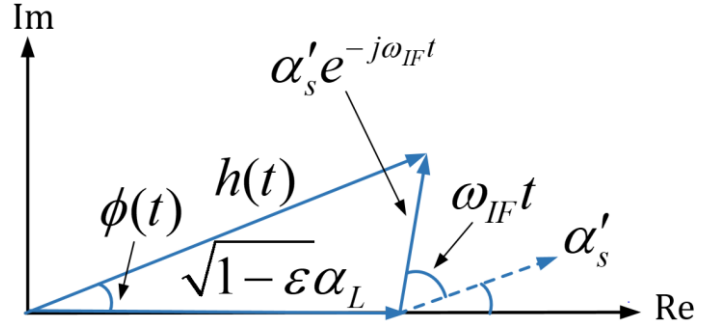


Fig. 3. The relationship between the retrieved α'_s and $h(t)$ for KK detection under the condition that $\varepsilon \rightarrow 1$.

Considering the signal and its image, as well as their corresponding vacuum fluctuations brought by the carrier, we have $\hat{h} = \sqrt{1-\varepsilon}(\hat{A}_L + \hat{A}'_s + \hat{A}'_i) + \sqrt{\varepsilon}(\hat{A}_s + \hat{A}_i)$ ($\varepsilon \rightarrow 1$) [11] before the PD port as shown in Fig. 2. (c).

Note that $I(t)$ corresponds to the photocurrent expectation $\langle \hat{I}(t) \rangle_{KK}$, which is obtained by projection via the coherent states, product states of the LO and the signal (and its image) states.

$$\begin{aligned} \langle \hat{I}(t) \rangle_{KK} &= k \langle \hat{h}^\dagger \hat{h} \rangle = k \langle \alpha_L | \langle \alpha_s | \langle \alpha_i | \hat{h}^\dagger \hat{h} | \alpha_i \rangle | \alpha_s \rangle | \alpha_L \rangle \\ &= k [\varepsilon \langle n_s \rangle + (1-\varepsilon) \langle n_L \rangle \\ &\quad + 2\sqrt{\varepsilon(1-\varepsilon)} |\alpha_s \alpha_L^*| \cos(\omega_{IF}t - \arg(\alpha_s \alpha_L^*))] \end{aligned} \quad (9)$$

The mean variance of the photocurrent is given by

$$\begin{aligned} \langle (\Delta \hat{I}(t))^2 \rangle_{KK} &= \langle \hat{I}(t)^2 \rangle - \langle \hat{I}(t) \rangle^2 \\ &= 2k^2 [\varepsilon \langle n_s \rangle + (1-\varepsilon) \langle n_L \rangle \\ &\quad + 2\sqrt{(1-\varepsilon)\varepsilon} |\alpha_s \alpha_L^*| \cos(\omega_{IF}t - \arg(\alpha_s \alpha_L^*))] \end{aligned} \quad (10)$$

The fluctuations of the photon current are related to the operators $\hat{A}_i \hat{A}_i^\dagger$, $\hat{A}_s \hat{A}_s^\dagger$ and $\hat{A}_L \hat{A}_L^\dagger$, which are in reverse order to the photon number operator. It is worth noting that the ratio of $\langle (\Delta \hat{I}(t))^2 \rangle_{KK}$ to $\langle \hat{I}(t) \rangle_{KK}$ is a constant $2k$. A general mathematical proof is given in the Appendix.

The operator $\Delta\hat{\phi}(t)$ representing the difference between the measured phase $\hat{\phi}(t)$ and the expected phase $\phi(t)$ is expressed by Eq. (11), which is obtained after Taylor expansion and approximation of the logarithm function in Eq. (6).

$$\Delta\hat{\phi}(t) = \hat{\phi}(t) - \phi(t) \approx \frac{1}{2\pi} \mathcal{P} \int_{-\infty}^{+\infty} \frac{1}{t-t'} \left[\frac{\hat{I}(t') - I(t')}{I(t')} \right] dt' . \quad (11)$$

The phase fluctuations $\langle(\Delta\hat{\phi}(t))^2\rangle$ can be expressed in discrete form with $t = l\delta t$, $t' = m\delta t$ and $dt' \rightarrow \delta t$.

$$\begin{aligned} \langle(\Delta\hat{\phi}(t))^2\rangle &= \lim_{\delta t \rightarrow 0} \frac{1}{4\pi^2} \left[\sum_{m=-\infty, m \neq l}^{m=+\infty} \langle(\Delta\hat{I}(m\delta t))^2\rangle / I(m\delta t)^2 / (l-m)^2 \right] \\ &= \lim_{\delta t \rightarrow 0} \frac{1}{12} \langle(\Delta\hat{I}(t))^2\rangle / (I(t))^2 = \frac{k}{6I(t)} \end{aligned} \quad (12)$$

(12)

δt is small enough to ensure that for each

$m, \langle(\Delta\hat{I}(m\delta t))^2\rangle / I(m\delta t)^2$ can be seen as fixed in the interval $[(m-1)\delta t, m\delta t]$.

In the derivation of Eq. (12), the cross terms vanish due to the fact that $\Delta\hat{I}(m_1\delta t)$ and $\Delta\hat{I}(m_2\delta t)$ at different instants are irrelevant. Therefore, only the square terms remain. To get the final result of Eq. (12), Eqs. (9) and (10) are applied and the fact that $\sum_{m=1}^{+\infty} 1/m^2 = \pi^2/6$ and $1/I(t)$ is continuous and derivative are considered. A detailed derivation of Eq.(12) is given in the Appendix.

Assuming the “ \parallel ” and “ \perp ” respectively represent the radical and tangential components, then $\langle(\Delta\hat{h}_{\parallel})^2\rangle$ and $\langle(\Delta\hat{h}_{\perp})^2\rangle$, which are the two orthogonal components of the radical (amplitude) and the tangential fluctuations of $h(t)$, correspondingly have the form $\Delta\hat{h}_{\parallel} = \Delta|\hat{h}(t)|$ and $\Delta\hat{h}_{\perp} = |\hat{h}(t)|\Delta\hat{\phi}(t)$ as shown in Fig. 4(a). We thus obtain the following quantum mechanical variances.

$$\begin{aligned} \langle(\Delta\hat{h}_{\parallel})^2\rangle &= \langle(\Delta|\hat{h}(t)|)^2\rangle = \langle[\sqrt{\hat{I}(t)} - \sqrt{I(t)}]^2\rangle / k \\ &\approx \langle\left[\frac{\hat{I}(t) - I(t)}{2\sqrt{I(t)}}\right]^2\rangle / k = \frac{\langle(\Delta\hat{I}(t))^2\rangle}{4kI(t)} = \frac{1}{2}, \end{aligned} \quad (13)$$

$$\langle(\Delta\hat{h}_{\perp})^2\rangle = \langle I(t)(\Delta\hat{\phi}(t))^2\rangle / k = \frac{\langle(\Delta\hat{I}(t))^2\rangle}{12kI(t)} = \frac{1}{6}. \quad (14)$$

From Eq. (8), the quantum fluctuations of α'_s are calculated as

$$\begin{aligned} N &= \langle(\Delta\hat{\alpha}'_s)^2\rangle \\ &= \langle(\Delta\hat{h})^2\rangle |e^{j\omega_{RF}t}|^2 = \langle(\Delta\hat{h}_{\parallel})^2\rangle + \langle(\Delta\hat{h}_{\perp})^2\rangle = \frac{2}{3}. \end{aligned} \quad (15)$$

Considering Eq. (15), the upper limit of S/N of KK detection

due to the quantum fluctuation is equal to $\frac{3}{2}\langle n_s \rangle$.

$$(S/N)_{KK} = \langle n_s \rangle / N = \frac{3}{2}\langle n_s \rangle. \quad (16)$$

In contrast, for the balanced heterodyne detection, under the same condition that $\langle n_L \rangle \gg \langle n_s \rangle$, the $(S/N)_{Bal}$ of approaches $\langle n_s \rangle$ as shown in Eq. (5).

From Eqs. (13) and (14) we find that, with the KK relations, \hat{h}_{\parallel} has the radical fluctuations twice that of a coherent state,

which embodies the contribution of the signal \hat{A}_s as well as the image \hat{A}_i . Meanwhile, the tangential fluctuations resulted by KK detection are only 1/3 times the radical ones. This ratio reveals the physical contribution of KK relation, which is, physically, from the Hilbert transform. The introduction of the Hilbert transform provides extra information for measuring the tangential component of the minimum-phase signal compared with direct measurement.

It is the smaller tangential fluctuation that leads to a greater signal-to-noise ratio of KK detection than balanced heterodyne detection.

The Arthurs-Kelly model [14] points out that, in order to realize the simultaneous measurement of a pair of non-reciprocal mechanical observables, two new reciprocal observables can be constructed, which have the same expected values as the former two do. Meanwhile, the total fluctuations resulted by the measurement process of the two observables constructed will be at least doubled compared with the respective measurement results of the two original observables. It can be proved that when $\langle n_L \rangle \gg \langle n_s \rangle$ holds, for the balanced heterodyne detection, as a pair of reciprocal observables constructed, the in-phase and quadrature components of $\hat{A}_s + \hat{A}_i^\dagger$ can be measured simultaneously, which contribute the same to the total fluctuations.

Different from the balanced heterodyne detection, for each symbol transmitted, KK receiver makes use of the detected photocurrent intensity information at each time in a symbol period, to indirectly measure (calculate) the heterodyne signal phase. Instead of measuring the tangential component physically, KK receiver utilizes the Kramers-Kronig constraint relations between the expected value of phase at the decision time $\phi(t)$, and that of photocurrent intensity at other times $I(t')$ ($-\infty < t' < +\infty, t' \neq t$) . This introduces more knowledge about phase $\phi(t)$ provided by the Hilbert transform, into the detection process, further compressing the fluctuations of phase measurement to only 1/3 times those of the amplitude. Eq. (15) reveals that, for KK receiver, the total quantum variance is only 2/3 compared with 1 of heterodyne detection, which indicates its physical nature.

Now for the specific frequency ω , we consider the original form of KK relations depicting the correlation between transmission for the intensity $\eta(\omega)$ and phase shift $\varphi(\omega)$ (with respect to propagation in the vacuum) of light which has propagated in the medium for a limited distance[15]. Comparing Eq. (6) with [15, Eq.(2)], it is obvious that in the sense of being linked by KK relations, $\eta(\omega)$ and $\varphi(\omega)$ respectively correspond to current $I(t)$ and its phase $\phi(t)$. Through the analysis in frequency domain, the conclusion of [15] is that compared with joint phase-loss estimation such as balanced heterodyne detection, the precision of measuring the phase shift can be further improved taking into account KK relations. This is consistent with our conclusion, that is, through the KK receiver, the amplitude and phase of minimum phase signal can be obtained at the same time, while the fluctuation of measuring phase can be

compressed to 1/6, which is even less than 1/4 of directly measuring phase component of a coherent state signal. This further leads to the result that using KK relations, the signal-to-noise ratio of coherent state signals can achieve $\frac{3}{2}\langle n_s \rangle$, which is higher than $\langle n_s \rangle$ of balanced heterodyne detection.

As shown in Fig. 4(b) and 4(c), the KK receiver results in a smaller total noise energy than the general heterodyne detection does, while the end point of the SSB signal from the KK receiver has an elliptical asymmetric distribution, indicating a specific physical essence of KK detection in quantum case.

Now we check the quantum variances of the in-phase and quadrature field operators of the signal $\langle(\Delta\hat{\alpha}'_{s1})^2\rangle$ and $\langle(\Delta\hat{\alpha}'_{s2})^2\rangle$, which represent the variances of amplitude and phase quadratures (position and momentum) of $\hat{\alpha}'_s$ respectively. From Fig. 3, by expanding $\Delta\hat{\alpha}'_s$ and $\Delta\hat{h}$, we can rewrite Eq. (8) as

$$\Delta\hat{\alpha}'_{s1} + j\Delta\hat{\alpha}'_{s2} = (\Delta\hat{h}_\parallel \cos(\phi(t)) - \Delta\hat{h}_\perp \sin(\phi(t)))e^{j\omega_{IF}t} + j(\Delta\hat{h}_\parallel \sin(\phi(t)) + \Delta\hat{h}_\perp \cos(\phi(t)))e^{j\omega_{IF}t}. \quad (17)$$

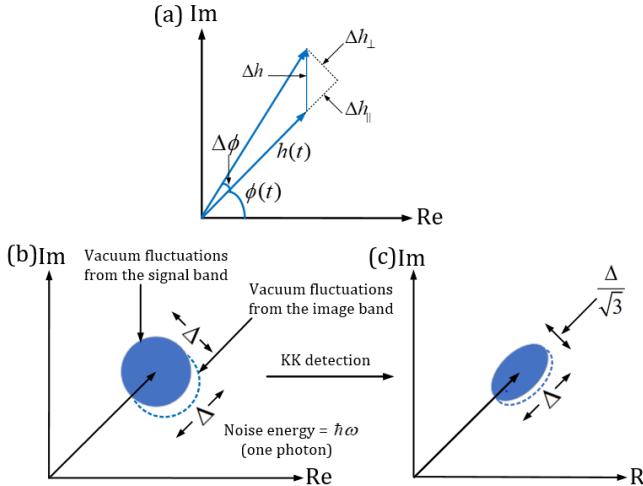


Fig. 4. Quantum noise associated with the KK receiver. (a) The radical and the tangential fluctuations; (b) Quantum noise from the signal and the image bands; (c) Phasor diagram of the light after KK detection. $\Delta = 1$ represents 2 times the standard deviation of the quantum fluctuations of the coherent state.

Substituting the relation $e^{j\omega_{IF}t} = \cos\omega_{IF}t + j\sin\omega_{IF}t$ into Eq.(17) to extract the real and the imaginary parts respectively, we get

$$\begin{bmatrix} \Delta\hat{\alpha}'_{s1} \\ \Delta\hat{\alpha}'_{s2} \end{bmatrix} = \begin{bmatrix} \cos(\omega_{IF}t + \phi(t)) & -\sin(\omega_{IF}t + \phi(t)) \\ \sin(\omega_{IF}t + \phi(t)) & \cos(\omega_{IF}t + \phi(t)) \end{bmatrix} \begin{bmatrix} \Delta\hat{h}_\parallel \\ \Delta\hat{h}_\perp \end{bmatrix}. \quad (18)$$

Then the variances of $\langle(\Delta\hat{\alpha}'_{s1})^2\rangle$ and $\langle(\Delta\hat{\alpha}'_{s2})^2\rangle$ are calculated as

$$\begin{bmatrix} \langle(\Delta\hat{\alpha}'_{s1})^2\rangle \\ \langle(\Delta\hat{\alpha}'_{s2})^2\rangle \end{bmatrix} = \begin{bmatrix} \cos^2(\omega_{IF}t + \phi(t)) & \sin^2(\omega_{IF}t + \phi(t)) \\ \sin^2(\omega_{IF}t + \phi(t)) & \cos^2(\omega_{IF}t + \phi(t)) \end{bmatrix} \begin{bmatrix} \langle(\Delta\hat{h}_\parallel)^2\rangle \\ \langle(\Delta\hat{h}_\perp)^2\rangle \end{bmatrix}. \quad (19)$$

To obtain Eq. (19), the relation $\langle\Delta\hat{h}_\parallel\Delta\hat{h}_\perp\rangle = 0$ is used.

Note that 'T' stands for matrix transposition. Eq. (19) shows that $\langle(\Delta\hat{\alpha}'_{s1})^2\rangle, \langle(\Delta\hat{\alpha}'_{s2})^2\rangle$ are related to $\langle(\Delta\hat{h}_\parallel)^2\rangle, \langle(\Delta\hat{h}_\perp)^2\rangle$ through a transformation matrix determined by $\omega_{IF}t + \phi(t)$, which brings no discrepancy between the fluctuation distributions of $\hat{\alpha}'_s$ and \hat{h} . As shown in Eq. (13) and Eq. (14), three times difference between $\langle(\Delta\hat{h}_\parallel)^2\rangle$ and $\langle(\Delta\hat{h}_\perp)^2\rangle$ results in the asymmetric distribution of $\langle(\Delta\hat{\alpha}'_s)^2\rangle$. For the retrieved $\hat{\alpha}'_s$, with the total fluctuations kept the same as those of \hat{h} , the in-phase and quadrature fluctuations both have a time dependent evolution as a function of $\omega_{IF}t + \phi(t)$. In other words, there exists a time varying accuracy for the measured position and momentum components of a coherent signal using KK receiver. From Fig.3, we can see that for a given α_s , the time varying of the projected in-phase and quadrature field fluctuation is related to the phase evolution of $\omega_{IF}t$.

For instance, Fig. 5 shows the phasor diagram of the retrieved signal α'_s at four specific orientations for a coherent state. In contrast to the conventional balanced heterodyne or homodyne detection, the KK receiver exhibits asymmetric quantum noise in both in-phase and quadrature operators that depends on the time varying phase of $\omega_{IF}t + \phi(t)$ when it is applied to measure a coherent state.

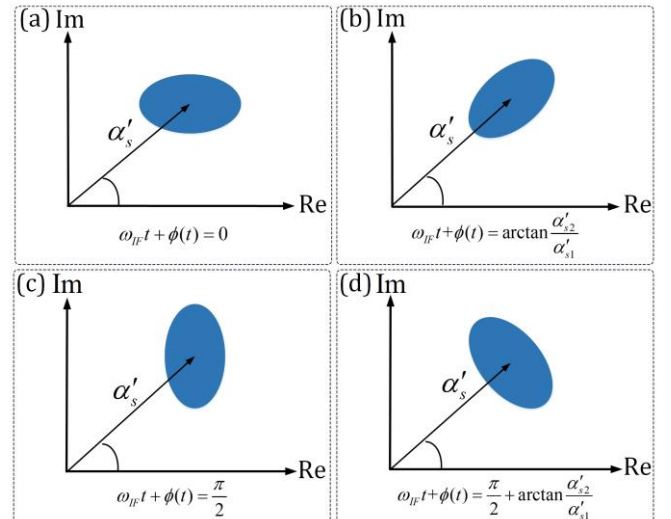


Fig. 5. Phasor diagram of the retrieved signal α'_s at four specific orientations for a coherent state.

Combing Fig. 3 and Fig.5, it can be seen that when $\sqrt{1-\varepsilon}\alpha_L \gg \alpha_s$ holds, there will hold $\phi(t) \approx 0$ no matter how t varies. Consequently, the phase term $\omega_{IF}t + \phi(t)$ will be approximately equal to $\omega_{IF}t$. Since here t is defined as the decision time while ω_{IF} represents the intermediate frequency, both of which are known varieties. In principle, we can control the fluctuation distribution by reasonably selecting these two variables. Thus, the fluctuation in the direction that needs to be

measured more accurately can be compressed to 1/6 equivalent to $\langle(\Delta\hat{h}_\perp)^2\rangle$. In the next part, taking the scenario of $\langle n_s \rangle = 100$ as an example, the results in Fig. 5 will be validated by numerical simulation.

5. SIMULATION RESULTS

To implement the minimum phase signal $h(t) = [\sqrt{1-\varepsilon}\alpha_L + \sqrt{\varepsilon}\alpha_s(t)e^{-j\omega_{IF}t}]e^{-j\omega_L t}$ in simulation, the key is how to set $\sqrt{1-\varepsilon}\alpha_L$, $\sqrt{\varepsilon}\alpha_s(t)$, ω_{IF} and ω_L . Considering that the factor $e^{-j\omega_L t}$ will be eliminated when $h(t)$ is converted into current as $k|h(t)|^2$, we have omitted this factor in simulation. Without losing generality, for each transmitted symbol, the terms $\sqrt{1-\varepsilon}\alpha_L$ and $\sqrt{\varepsilon}\alpha_s(t)$, with t defined as the decision time point, are both set as constant values. Based on this assumption, the power ratio of carrier to signal (CSPR) of the minimum-phase signal can be defined as

$$CSPR \triangleq \frac{|\sqrt{1-\varepsilon}\alpha_L|^2}{|\sqrt{\varepsilon}\alpha_s(t)|^2} = \frac{(1-\varepsilon)\langle n_L \rangle}{\varepsilon\langle n_s \rangle} > 1.$$

As for the representation of intermediate frequency ω_{IF} , the period corresponding to ω_{IF} is defined as T_{IF} , which can be represented as $\omega_{IF}T_{IF} = 2\pi$. The T_{IF} should correspond to a sufficient number of sampling points, which is set as 2000 in our simulation. It is to meet the condition that the time interval between each two sampling points approaches zero, which is represented as $\delta t \rightarrow 0$ in Eq.(12), & (B2)-(B4).

To approximate the KK relations, Eq.(6) is discretized into the form of Riemannian sum. The integral interval of Eq.(6) is $(-\infty, +\infty)$, which is physically impossible. In practice, time 0 is selected as the starting point of integration, with T selected as the total integral interval. Then the decision time t in Eq. (6) is set at $T/2$, which ensures that the integral intervals on both sides of the singularity are selected almost symmetrical. Up to 2×10^5 sampling points are selected for T , which means that $\delta t = T/(2 \times 10^5)$. This ensures that T is set large enough to approximate the integral interval $(-\infty, +\infty)$. While the decision time t is selected as the 10^5 th sampling point, which also corresponds to the singularity of the principal value integral in Eq. (6).

To illustrate the distribution of received symbols on the constellation plane and show the statistical nature of fluctuations, up to 40000 symbols are transmitted each time. Without losing generality, the QPSK modulation format is selected in the simulation for simplicity.

In order to keep the noise properties resulted by quantum fluctuations in simulation consistent with the physical conditions, the measurement at each time point should obey the Poisson distribution, while the optical impulse noise should conform to the properties of Gaussian white noise. Since the

Poisson distribution can be approximated by Gaussian distribution as its mean becomes large[16], Gaussian random number is used to simulate measurement noise. At the same time, by adding current noise at each time point independently, the Gaussian white noise property is satisfied. Thus to model the fluctuations of current $\langle(\Delta\hat{I}(t))^2\rangle_{KK}$, as has been proved in the appendix Eq.(A5), we may as well assume that the current deviation $\Delta I(t)_{KK}$ has the following form for carrying out the simulation using Matlab.

$$\Delta I(t)_{KK} = \sqrt{2k\langle\hat{I}(t)\rangle_{KK}} \times \text{randn} \quad (20)$$

Where 'randn' represents the Gaussian random number with the mean value as 0 and the standard deviation as 1, thus the quantum noise of $I(t)_{KK}$ at time point t is modeled as the independent Gaussian noise with 0 mean and variance equaling to $2k\langle\hat{I}(t)\rangle_{KK}$.

Therefore, the form of, as shown in (20), can make the noise in the simulation close to the real situation.

First, we set CSPR to 10dB and let $\langle n_s \rangle$ start from 20 and increase in a step of 20. The received constellations with $\langle n_s \rangle = 60, 100, 160, 200$ are respectively shown in Fig.6.

For QPSK modulation format, it can be seen that the fluctuations surrounding each constellation point showed an asymmetric elliptical distribution on the constellation plane.

With $\langle n_s \rangle$ increasing, the fluctuations surrounding each constellation point decreases. Moreover, the fluctuations present an ellipse distribution as we have predicted in pre-sections. The analysis results for the constellations with $csp = 10\text{dB}$ & $\langle n_s \rangle$ varing from 20 to 200 are concluded in Fig. 7 (a) & Fig. 7. (b), where the square of the ratio of the major axis to the minor one of fluctuation ellipse is defined as ρ_{KK} .

Fig.7. (a) shows ρ_{KK} in four quadrants calculated by principal component analysis (PCA) method provided by Matlab. Fig.7. (b) shows the calulated signal-to-noise ratio (SNR) of the received QPSK signals based on KK receiver for different $\langle n_s \rangle$.

As shown in Fig.7. (a), the ρ_{KK} of the simulation results is almost consistent with the predicted value 3/1. While Fig. 7. (b) indicates that for KK receiver, the SNR of the signal is propotional to its photon number $\langle n_s \rangle$, which shows approximately a linear correlation of $SNR = \frac{3}{2}\langle n_s \rangle$. The simulative results of Fig.7 (a) and Fig.(b) are consistent with our conclusion represented by Eq.(13) & (14).

Fixing $\langle n_s \rangle$ as 100, Fig.8 illustrates the received constellation diagram with CSPR set as 5dB, 10dB, 15dB and 20dB, respectively.

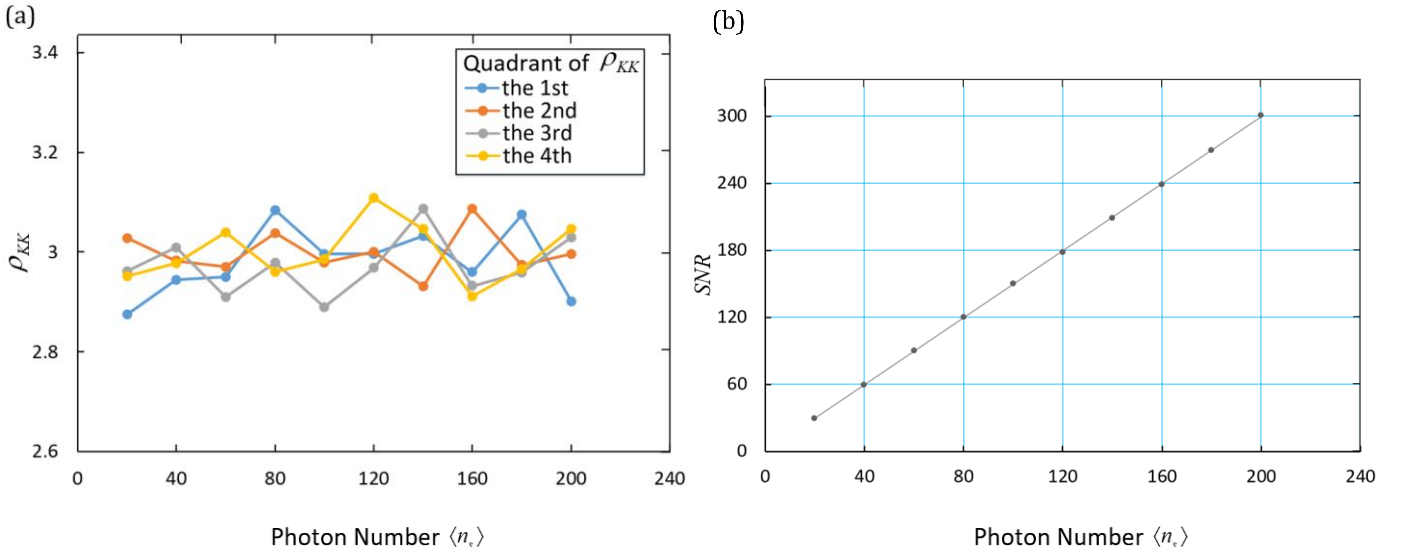


Fig. 7. The analysis results for the constellations with $CSPR = 10\text{dB}$ & $\langle n_s \rangle$ varing from 20 to 200.

(a) ρ_{KK} of each quadrant;(b)The Relation Between SNR and $\langle n_s \rangle$.

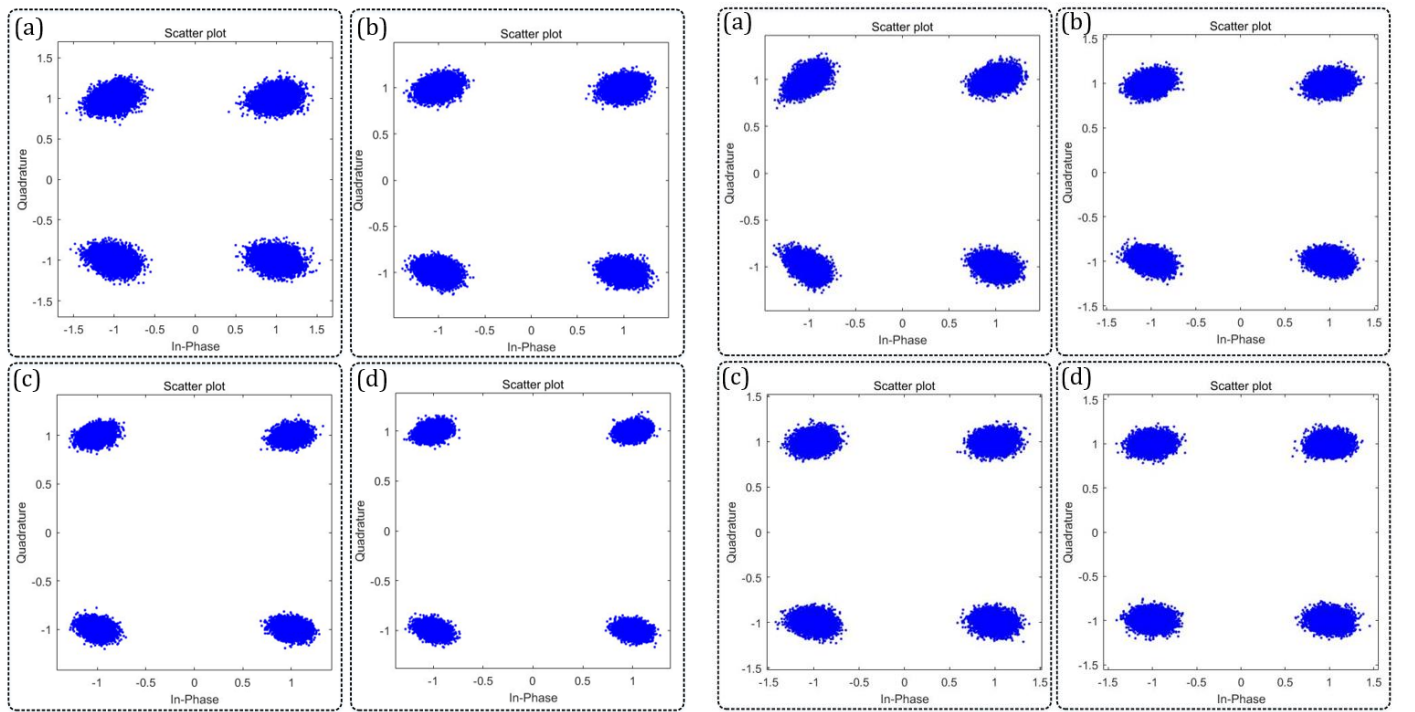


Fig. 6. The received constellations of different $\langle n_s \rangle$ with $CSPR = 10\text{dB}$.

(a) $\langle n_s \rangle = 60$; (b) $\langle n_s \rangle = 100$; (c) $\langle n_s \rangle = 160$; (d) $\langle n_s \rangle = 200$.

Fig. 8. The received constellations of different $CSPR$ with $\langle n_s \rangle = 100$

(a) $CSPR = 5\text{dB}$;(b) $CSPR = 10\text{dB}$;(c) $CSPR = 15\text{dB}$;(d) $CSPR = 20\text{dB}$

As shown in Fig. 8, with the CSPR increasing, the direction of the major axis of the fluctuation ellipse surrounding the constellation point of each quadrant, tends to be consistent with the direction of the carrier as predicted at the end of Section IV. This implies that when the CSPR is large enough ($(1-\varepsilon)\langle n_s \rangle \gg \varepsilon\langle n_s \rangle$ holds), the distribution of the fluctuations will be determined by the carrier phase almost completely.

For the simulation of the four cases predicted in Fig. 5, the CSPR is set as 30dB to meet the condition

$(1-\varepsilon)\langle n_s \rangle \gg \varepsilon\langle n_s \rangle$. The decision time t in Eq.(19) is selected with ω_{IF} fixed to meet the conditions $\omega_{IF}t \bmod T_{IF} = 0, \frac{\pi}{4}, \frac{\pi}{2}$ & $\frac{3\pi}{4}$, respectively.

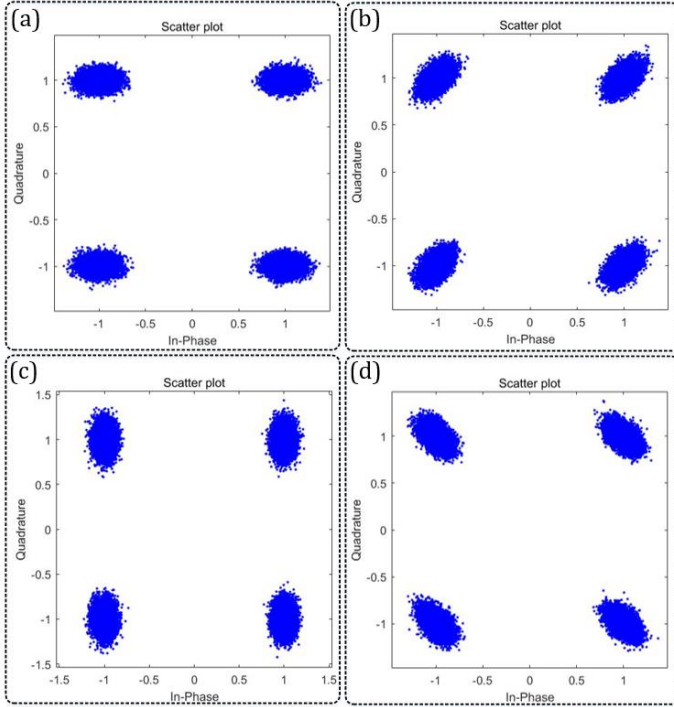


Fig. 9. The received constellations of different decision time t with $\langle n_s \rangle = 100$ and $CSPR = 30\text{dB}$

$$\begin{aligned}
 \text{(a)} \quad & \omega_{IF}t \bmod T_{IF} = 0; \\
 \text{(b)} \quad & \omega_{IF}t \bmod T_{IF} = \frac{\pi}{4}; \\
 \text{(c)} \quad & \omega_{IF}t \bmod T_{IF} = \frac{\pi}{2}; \\
 \text{(d)} \quad & \omega_{IF}t \bmod T_{IF} = \frac{3\pi}{4}
 \end{aligned}$$

Fig. 9(a)-(d) show the received constellations when the decision time t is selected as the above four values respectively, where the fluctuation distribution result of each case corresponds to that one predicted in Fig. 5(a)-(d). As shown in the case of Fig. 9. (a) and Fig. 9. (c), we can respectively compress the in-phase or quadratic fluctuation to only 1/6 while keeping that of the other direction to 1/2. In Fig. 9. (b) and Fig. 9. (d), the fluctuation of both in-phase and quadratic components can be compressed to 1/3 at the same time. The results indicate that for high CSPR such as $CSPR \geq 30\text{dB}$, the KK receiver can achieve a high controllability of the fluctuation distribution on the constellation plane. This is implemented by selecting the phase term $\omega_{IF}t$ according to the requirements of measurement accuracy varying with the two orthogonal directions to be measured.

6. CONCLUSION

In summary, we analytically derive the quantum noise of the in-phase and quadrature operators of the retrieved signal with the KK receiver. The analytical conclusions are validated by numerical simulation. The quantum limit of the S/N of the KK receiver is 3/2 times the expectation value of the signal photon number. Therefore, the KK receiver has a larger S/N limit than that of heterodyne detection, which has an uncertainty product 3-dB larger than the one dictated by the uncertainty principle. This is consistent with the conclusion of [15]. Since the intensity of the SSB signal is physically

measured, while its phase is calculated from the intensity using Kramers-Kronig relations, KK receiver keeps the tangential noise to 1/3 times that of the amplitude, leading to an asymmetric distribution of the quantum fluctuation of the retrieved signal. The projected variances of the in-phase and quadrature operators are time-varying due to the phase evolution of the intermediate frequency, which provides us a scheme using a high CSPR to measure the component of a specific direction with fluctuations compressed to 1/6. Our work provides a physical insight of the KK receiver and should enrich the knowledge of electromagnetic noise in quantum optical measurement.

Funding.

National Natural Science Foundation of China (62271010, U21A20454 and 11834010); National Key Research and Development Program of China (2018YFB1801204 and 2016YFA0301402).

Acknowledgment.

REFERENCES

1. Kazuro Kikuchi, "Fundamentals of coherent optical fiber communications," *J. Lightwave Technol.* **34**, 157-179 (2016).
2. Antonio Mecozzi, Cristian Antonelli, and Mark Shtaif, "Kramers-Kronig coherent receiver," *Optica* **3**, 1220-1227 (2016).
3. Antonio Mecozzi, Cristian Antonelli, and Mark Shtaif, "Kramers-Kronig receivers," *Adv. Opt. Photon.* **11**, 480-517 (2019).
4. X. Chen, C. Antonelli, S. Chandrasekhar, G. Raybon, A. Mecozzi, M. Shtaif, and P. Winzer, "Kramers-Kronig receivers for 100-km datacenter interconnects," *J. Lightwave Technol.* **36**, 79 – 89 (2018).
5. S. T. Le, K. Schuh, R. Dischler, F. Buchali, L. Schmalen, and H. Buelow, "Beyond 400 Gb/s direct detection over 80 km for data center Zinterconnect applications," *J. Lightwave Technol.* **38**, 538-545 (2020).
6. Braunstein, Samuel L. and van Loock, Peter, "Quantum information with continuous variables," *Rev. Mod. Phys.* **77**, 513-577 (2005).
7. G. Adesso and F. Illuminati, "Entanglement in continuous-variable systems: recent advances and current perspectives," *J. Phys. A: Math. Theor.* **40**, 7821-7880 (2007).
8. X.-B. Wang, T. Hirashima, A. Tomita, and M. Hayashi, "Quantum information with Gaussian states," *Phys. Rep.* **448**, 1-111 (2007).
9. C. Weedbrook, S. Pirandola, R. García-Patrón, N. J. Cerf, T. C. Ralph, J. H. Shapiro, and S. Lloyd, "Gaussian quantum information," *Rev. Mod. Phys.* **84**, 621-669 (2012).
10. X. Su, M. Wang, Z. Yan, X. Jia, C. Xie, and K. Peng, "Quantum network based on non-classical light," *Sci. China Inf. Sci.* **63**, 180503 (2020).
11. Y. Yamamoto and H. A. Haus, "Preparation, measurement and information capacity of optical quantum states," *Rev. Mod. Phys.* **58**, 1001—1020 (1986).
12. M. O. Scully and M. S. Zubairy, "quantum phase and amplitude fluctuations," in *Quantum Optics* (Cambridge University Press, 1997), Ch. XIV, pp. 423-426.
13. H. A. Haus, "Detection," in *Electromagnetic Noise and Quantum Optical Measurements* (Berlin Heidelberg, Springer-Verlag, 2000), Ch. VIII, pp. 281-304.
14. E. Arthurs and J. L. Kelly, "B.S.T.J. briefs: on the simultaneous measurement of a pair of conjugate observables," *The Bell System Technical Journal* **44**, 725-729 (1965).
15. Ilaria Gianani, Francesco Albarelli, Adriano Verna, Valeria Cimini, Rafal Demkowicz-Dobrzanski, and Marco Barbieri, "Kramers-Kronig relations and precision limits in quantum phase estimation," *Optica* **8**, 1642-1645 (2021).
16. Feller W., "laws of large numbers," in *An Introduction to Probability Theory and its Applications*, 3rd ed. (John Wiley & Sons, Inc, 1968), Vol. I, Ch. X, pp. 245-246.

Supplementary Materials

APPENDIX A: THE GENERAL PROOF OF THE RELATION OF EQ. (9) AND EQ. (10)

Here we give a general proof of the relation of Eq.(9) and Eq.(10) in the main text. Considering an operator \hat{I} that measures the intensity of the electrical field consisting of N different frequency modes \hat{A}_u ($u=1, \dots, N$), we have

$$\hat{I} = \left(\sum_{u=1}^N \lambda_u \hat{A}_u \right)^\dagger \left(\sum_{u=1}^N \lambda_u \hat{A}_u \right). \quad (\text{A1})$$

λ_u is the strength of \hat{A}_u . We have the following commutation relation as

$$\sum_{u=1}^N \lambda_u^2 = \left[\left(\sum_{u=1}^N \lambda_u \hat{A}_u \right), \left(\sum_{u=1}^N \lambda_u \hat{A}_u \right)^\dagger \right] = r. \quad (\text{A2})$$

Considering the expression that the operator \hat{I}^2 minus the normally ordered operator of \hat{I}^2 , we have

$$\begin{aligned} \hat{I}^2 - : \hat{I}^2 : &= \left[\left(\sum_{u=1}^N \lambda_u \hat{A}_u \right)^\dagger \left(\sum_{u=1}^N \lambda_u \hat{A}_u \right) \right]^2 \\ &\quad - \left[\left(\sum_{u=1}^N \lambda_u \hat{A}_u \right)^\dagger \right]^2 \left[\left(\sum_{u=1}^N \lambda_u \hat{A}_u \right) \right]^2 \\ &= \left(\sum_{u=1}^N \lambda_u \hat{A}_u \right)^\dagger \left[\left(\sum_{u=1}^N \lambda_u \hat{A}_u \right), \left(\sum_{u=1}^N \lambda_u \hat{A}_u \right)^\dagger \right] \left(\sum_{u=1}^N \lambda_u \hat{A}_u \right) \\ &= \left(\sum_{u=1}^N \lambda_u \hat{A}_u \right)^\dagger \left(\sum_{u=1}^N [\hat{A}_u, \hat{A}_u^\dagger] \lambda_u^2 \right) \left(\sum_{u=1}^N \lambda_u \hat{A}_u \right) \\ &= r \left(\sum_{u=1}^N \lambda_u \hat{A}_u \right)^\dagger \left(\sum_{u=1}^N \lambda_u \hat{A}_u \right) \end{aligned} \quad (\text{A3})$$

Here $: \hat{I}^2 :$ represents the normally ordered \hat{I}^2 only including the terms with the creation operators preceding the annihilation operators.

The expectation of $\hat{I}^2 - : \hat{I}^2 :$ equals to the fluctuations $\langle (\Delta \hat{I})^2 \rangle$ in the measurement of \hat{I} . We have

$$\begin{aligned} \langle (\Delta \hat{I})^2 \rangle &= \langle \hat{I}^2 - : \hat{I}^2 : \rangle \\ &= r \langle \left(\sum_{u=1}^N \lambda_u \hat{A}_u \right)^\dagger \left(\sum_{u=1}^N \lambda_u \hat{A}_u \right) \rangle. \end{aligned} \quad (\text{A4})$$

As for $\hat{h} = \sqrt{1-\varepsilon}(\hat{A}_L + \hat{A}_s' + \hat{A}_i') + \sqrt{\varepsilon}(\hat{A}_s + \hat{A}_i)$ ($\varepsilon \rightarrow 1$) in our paper, we have $N = 5$ and $r = \sum_{u=1}^N \lambda_u^2 = 3(1-\varepsilon) + 2\varepsilon = 3 - \varepsilon \rightarrow 2$.

Therefore, for $\hat{I}(t)_{KK} = k \hat{h}^\dagger \hat{h}$, we obtain

$$\langle (\Delta \hat{I}(t))^2 \rangle_{KK} = 2k \langle \hat{I}(t) \rangle_{KK}. \quad (\text{A5})$$

Eq. (10) in the main text can thus be readily obtained from Eq. (9) through the relation that is revealed in Eq. (A5).

APPENDIX B: THE DERIVATION OF EQ. (12)

Here we give the derivation of Eq. (12) in the main text. Note that Eq.(11) can be used to calculate the phase fluctuations.

$$\langle (\Delta \hat{\phi}(t))^2 \rangle = \frac{1}{4\pi^2} \left\langle \left\{ \mathcal{P} \int_{-\infty}^{+\infty} \frac{1}{t-t'} \left[\frac{\hat{I}(t') - I(t')}{I(t')} \right] dt' \right\}^2 \right\rangle \quad (\text{B1})$$

Let $t = l\delta t$, $t' = m\delta t$ and $dt' \rightarrow \delta t$, then Eq.(B1) can be rewritten as the following discrete form. To bypass the singularity of the integrand, $m \neq l$.

$$\langle (\Delta \hat{\phi}(t))^2 \rangle = \lim_{\delta t \rightarrow 0} \frac{1}{4\pi^2} \left\langle \left\{ \sum_{m=-\infty, m \neq l}^{m=+\infty} \frac{1}{l\delta t - m\delta t} \left[\frac{\Delta \hat{I}(m\delta t)}{I(m\delta t)} \right] \right\}^2 (\delta t)^2 \right\rangle \quad (\text{B2})$$

Due to the white noise property, the measurement of $\Delta \hat{I}$ at different instants $m_1 \delta t$ and $m_2 \delta t$ are irrelevant. Considering the cross terms in the summation in Eq.(B2), we have

$$\begin{aligned} &\lim_{\delta t \rightarrow 0} \frac{1}{4\pi^2} \left\langle \sum_{m_1, m_2} \frac{1}{(l-m_1)(l-m_2)} \frac{\Delta \hat{I}(m_1 \delta t) \Delta \hat{I}(m_2 \delta t)}{I(m_1 \delta t) I(m_2 \delta t)} \right\rangle \\ &= \lim_{\delta t \rightarrow 0} \frac{1}{4\pi^2} \sum_{m_1, m_2} \frac{1}{(l-m_1)(l-m_2)} \frac{\langle \Delta \hat{I}(m_1 \delta t) \rangle \langle \Delta \hat{I}(m_2 \delta t) \rangle}{I(m_1 \delta t) I(m_2 \delta t)} \\ &= 0 \end{aligned} \quad (\text{B3})$$

Therefore, the cross terms vanish and only the square terms remain. We can thus rewrite $\langle (\Delta \hat{\phi}(t))^2 \rangle$ as

$$\begin{aligned} \langle (\Delta \hat{\phi}(t))^2 \rangle &= \lim_{\delta t \rightarrow 0} \frac{1}{4\pi^2} \left[\sum_{m=-\infty}^{m=l-1} \frac{1}{(l-m)^2} \frac{\langle (\Delta \hat{I}(m\delta t))^2 \rangle}{I(m\delta t)^2} \right. \\ &\quad \left. + \sum_{m=l+1}^{+\infty} \frac{1}{(l-m)^2} \frac{\langle (\Delta \hat{I}(m\delta t))^2 \rangle}{I(m\delta t)^2} \right]. \end{aligned} \quad (\text{B4})$$

We introduce Eq. (9) and Eq. (10) in the main text into Eq. (B4) and consider Eq. (A5) in the derivation of Eq. (12) in the main text.

Note that $\sum_{m=1}^{+\infty} 1/m^2 = \pi^2/6$, the final result of Eq. (12) in the main text is thus obtained.